Cationic M(II)/Co(0) (M = Pd, Pt) Metallomacrocycles Containing Tetrahedral Co_2C_2 Cluster Cores Formed by Self-Assembly of Cluster-Bridged Bipyridine $(4\text{-}C_5H_4NCO_2CH_2)_2C_2Co_2(CO)_6$ and Diarsine-Chelated Complex $[Pd(dpab)(H_2O)(OTf)][OTf]$ or $[Pt(dpab)(H_2O)_2][OTf]_2$

Li-Cheng Song,* Guo-Xia Jin, Wen-Xiong Zhang, and Qing-Mei Hu

Department of Chemistry, State Key Laboratory of Elemento-Organic Chemistry, Nankai University, Tianjin 300071, People's Republic of China

Received October 24, 2004

The synthesis, characterization, and some reactions of the tetrahedral Co_2C_2 cluster-bridged bipyridine $(4\text{-}C_5H_4NCO_2CH_2)_2C_2Co_2(CO)_6$ (**2**) and the diarsine-chelated complexes $Pd(dpab)Cl_2$ (**3**, dpab = 1,4-bis(diphenylarsino)butane), $[Pd(dpab)(H_2O)(OTf)][OTf]$ (**4**, OTf = SO_3CF_3), $Pt(dpab)Cl_2$ (**5**), and $[Pt(dpab)(H_2O)_2][OTf]_2$ (**6**) have been investigated. While the bridged bipyridine **2** could be prepared by reaction of 4-pyridinecarboxylic acid 2-butyne-1,4-diyl ester **1** with $Co_2(CO)_8$ in 86% yield, the chelated dichloride complexes **3** and **5** were obtained by reaction of K_2PdCl_4 or $(PhCN)_2PtCl_2$ with dpab in 90% and 77% yields. Further reactions of **3** and **5** with silver triflate followed by treatment with water afforded the corresponding chelated aqua/triflate complexes **4** and **6** in 92% and 88% yields. More interestingly, **4** and **6** were found to undergo self-assembly with **2** to give two cationic metallomacrocycles $\{[M(dpab)]\text{-}\mu\text{-}[(4\text{-}C_5H_4NCO_2CH_2)_2C_2Co_2(CO)_6]\}_2[OTf]_4$ (**7**, M = Pd; **8**, M = Pt) in 92% and 85% yields. X-ray crystal structures were determined for the Co_2C_2 cluster-containing metallomacroycles **7** and **8**, as well as bipyridine **2** and complexes **4** and **6**.

Introduction

It is well-known that metallomacrocycles are an important class of metal-containing compounds that have been involved in modern supramolecular chemistry with unique structures and novel properties.[1−3] On the other hand, it is also known that self-assembly is one of the most practical methodologies for synthesis of metallomacrocycles such as molecular squares,[4] rectangles,[5] parallelograms,[6] and rhomboids,[7] as well as those metallomacrocycles that contain the redox-active tetrahedral M_2FeS (M = Mo, W) cluster cores.[8] Since we are interested in cluster-containing macrocycles,[8,9] we recently initiated a study on self-assembly of the tetrahedral Co_2C_2 cluster-bridged bipyridine ligand $(4\text{-}C_5H_4NCO_2CH_2)_2C_2Co_2(CO)_6$ (**2**) with the dpab-chelated Pd(II) complex $[Pd(dpab)(H_2O)(OTf)][OTf]$ (**4**, dpab = 1,4-bis(diphenylarsino)butane; OTf = SO_3CF_3) or Pt(II) complex $[Pt(dpab)(H_2O)_2][OTf]_2$ (**6**), aimed to obtain the corresponding Co_2C_2 cluster-containing metallomacrocyclic compounds that may have unique structures and new properties. Now, we report our results.

Results and Discussion

Synthesis and Characterization of Tetrahedral Co_2C_2 Cluster-Bridged Bipyridine $(4\text{-}C_5H_4NCO_2CH_2)_2C_2Co_2(CO)_6$ (2). It was found that treatment of

* To whom correspondence should be addressed. Fax: 0086-22-23504853. E-mail: lcsong@nankai.edu.cn.

(1) Vögtle, F. *Supramolecular Chemistry, An Introduction*; Wiley: Chichester, 1991.

(2) Lehn, J.-M. *Supramolecular Chemistry*; *Concepts and Perspectives*; VCH: New York, 1995.

(3) Cram, D. J.; Cram, J. M. *Container Molecules and Their Guests*; The Royal Society of Chemistry: Cambridge, U.K., 1994.

(4) (a) Stang, P. J.; Cao D. H.; Saito, S.; Arif, A. M. *J. Am. Chem. Soc.* **1995**, *117*, 6273. (b) Stang, P. J.; Olenyuk, B.; Fan, J.; Arif, A. M. *Organometallics* **1996**, *15*, 904. (c) Fujita, M.; Yu, S.-Y.; Kusukawa, T.; Funaki, H.; Ogura, K.; Yamaguchi, K. *Angew. Chem., Int. Ed.* **1998**, *37*, 2082. (d) Stang, P. J.; Cao, D. H. *J. Am. Chem. Soc.* **1994**, *116*, 4981. (e) Fujita. M.; Kwon, Y. J.; Washizu, S.; Ogura, K. *J. Am. Chem. Soc*. **1994**, *116*, 1151. (f) Rauter, H.; Hillgeris, E. C.; Erxleben, A.; Lippert, B. *J. Am. Chem. Soc*. **1994**, *116*, 616. (g) Davies, S. C.; Duhme, A.-K.; Hughes, D. L. *Inorg. Chem*. **1998**, *37*, 5380. (h) Fujita. M.; Yazaki, J.; Ogura, K. *J. Am. Chem. Soc*. **1990**, *112*, 5645. (i) Stang, P. J.; Chen, K.; Arif, A. M. *J. Am. Chem. Soc*. **1995**, *117*, 8793. (j) Stang, P. J.; Chen, K. *J. Am. Chem. Soc*. **1995**, *117*, 1667.

(5) (a) Jeong, K.-S.; Cho, Y. L.; Song, J. U.; Chang, H.-Y.; Choi, M.-G. *J. Am. Chem. Soc*. **1998**, *120*, 10982. (b) Fujita, M. *Chem. Soc. Rev*. **1998**, *27*, 417. (c) Woessner, S. M.; Helms, J. B.; Shen, Y.; Sullivan, B. P. *Inorg. Chem*. **1998**, 37, 5406. (d) Benkstein, K. D.; Hupp, J. T.; Stern, C. L. *Inorg. Chem.* **1998**, *37*, 5404. (e) Benkstein, K. D.; Hupp, J. T.; Stern, C. L. *J. Am. Chem. Soc*. **1998**, *120*, 12982.

(6) (a) Habicher, T.; Nierengarten, J.-F.; Gramlich, V.; Diederich, F. *Angew. Chem., Int. Ed.* **1998**, *37*, 1916. (b) Fujita, M.; Aoyagi, M.; Ogura, K. *Inorg. Chim. Acta* **1996**, *246*, 53. (c) Hartshorn, C. M.; Steel, P. J. *Inorg. Chem*. **1996**, *35*, 6902.

(7) Schmitz, M.; Leininger, S.; Fan, J.; Arif, A. M.; Stang, P. J. *Organometallics* **1999**, *18*, 4817.

(8) (a) Song, L.-C.; Guo, D.-S.; Q.-M. Hu; Huang, X. Y. *Organometallics* **2000**, *19*, 960. (b) Song, L.-C.; Zhu, W.-F.; Hu, Q.-M. *Organometallics* **2002**, *21*, 5066.

(9) (a) Song, L.-C.; Fan, H.-T.; Hu, Q.-M. *J. Am. Chem. Soc*. **2002**, *124*, 4566. (b) Song, L.-C.; Fan, H.-T.; Hu, Q.-M.; Yang, Z.-Y.; Sun, Y.; Gong F.-H. *Chem. Eur. J.* **2003**, *9*, 170. (c) Song, L.-C.; Gong, F.-H.; Meng, T.; Ge, J.-H.; Cui, L.-N.; Hu Q.-M. *Organometallics* **2004**, *23*, 823. (d) Song, L.-C.; Guo, D.-S.; Hu, Q.-M.; Sun, J. *J. Organomet. Chem*. **2000**, *616*, 140. (d) Song, L.-C.; Guo, D.-S.; Hu, Q.-M.; Su, F.-H.; Sun, J.; Huang, X.-Y. *J. Organomet. Chem*. **2001**, *622*, 210.

10.1021/om049175y CCC: $30.25
Publication on Web 01/12/2005

Scheme 1

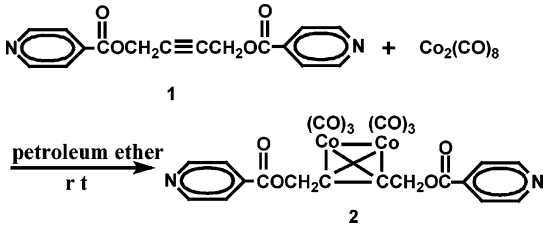

4-pyridinecarboxylic acid 2-butyne-1,4-diyl ester **1** with $Co_2(CO)_8$ in petroleum ether at room temperature for 2−3 h resulted in formation of the tetrahedral Co_2C_2 cluster-bridged bipyridine **2** in 86% yield (Scheme 1).

The bridged bipyridine **2** is the first bipyridine derivative containing a cluster core, which was fully characterized by elemental analysis, IR, ^{1}H NMR, ^{13}C NMR, and X-ray diffraction techniques. For example, the IR spectrum of **2** showed one absorption band at 1728 cm^{-1} for its ester carbonyl groups and four absorption bands in the range 2105−1993 cm^{-1} for its terminal carbonyls. In addition, the ^{1}H NMR spectrum of **2** displayed one singlet at 5.55 ppm for its CH_2 groups and two broad singlets at 9.18 and 7.95 ppm for its pyridine rings. The structure of **2** was unequivocally confirmed by X-ray crystallography. The ORTEP drawing of **2** is shown in Figure 1, while Table 1 lists its selected bond lengths and angles. The X-ray crystallography reveal that **2** is indeed a tetrahedral Co_2C_2 cluster-bridged bipyridine in which the C(14)−C(15) bond is essentially perpendicular to the Co(1)−Co(2) bond. In addition, the carbon chain of C(13)-through-C(16) is attached to O(7) and O(9) of the two 4-pyridine carboxylate units, whereas the two cobalt atoms Co(1) and Co(2) each are bound to three terminal carbonyls. The Co(1)−Co(2) (2.4817(9) Å) and C(14)−C(15) (1.343(3) Å) distances as well as the C(13)−C(14)−C(15) (139.6(2)°) and C(14)−C(15)−C(16) (141.2(2)°) angles are all comparable with those found for other tetrahedral Co_2C_2 systems.[10] More interestingly, this complex has been proved to be a very efficient ligand for self-assembly of the desired cluster-containing macrocycles (vide infra).

Synthesis and Characterization of dpab-Chelated Pd(II) Complexes Pd(dpab)Cl$_2$ (3) and [Pd(dpab)(H$_2$O)(OTf)][OTf] (4). We further found that reaction of K_2PdCl_4 with dpab in EtOH at room temperature for 12 h gave the Pd(II) dichloride complex **3** in 90% yield, whereas complex **3** reacted with silver triflate in CH_2Cl_2 at room temperature for 24 h followed by 10 min stirring in air to afford the Pd(II) monoaqua complex **4** in 93% yield (Scheme 2).

It is worth pointing out that the starting material dpab ligand was prepared by a new route. This route involves reaction of 1,4-dibromobutane with lithium followed by treatment of the intermediate $Li(CH_2)_4Li$ with Ph_2AsCl. This route has much higher yield (73% vs 15%) than that previously reported involving reaction of Ph_3As with potassium and subsequent treatment of the intermediate Ph_2AsK with 1,4-dichlorobutane.[11] In addition, it is believed[4a,b] that reaction of complex **3** with silver triflate might first give bis(triflate) complex Pd(dpab)(OTf)$_2$, and the monoaqua complex **4** was produced by hydrolysis of Pd(dpab)(OTf)$_2$ in the workup process with 10 min stirring in open air.

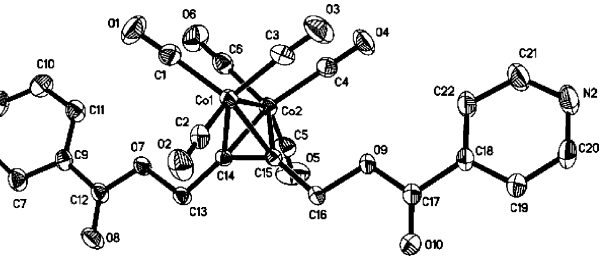

Figure 1. Molecular structure of **2** (thermal ellipsoids with 30% probability).

Table 1. Selected Bond Lengths (Å) and Angles (deg) for 2

Co(1)−C(14)	1.944(3)	N(1)−C(10)	1.320(4)
Co(1)−C(15)	1.952(3)	N(1)−C(8)	1.329(5)
Co(1)−Co(2)	2.4817(9)	C(12)−O(8)	1.200(3)
Co(2)−C(14)	1.951(2)	C(12)−O(7)	1.340(3)
Co(2)−C(15)	1.962(3)	C(14)−C(15)	1.343(3)
C(1)−Co(1)−C(14)	103.65(13)	C(10)−N(1)−C(8)	115.9(3)
C(14)−Co(1)−C(15)	40.34(10)	O(8)−C(12)−O(7)	123.9(3)
C(14)−Co(1)−Co(2)	50.53(7)	O(8)−C(12)−O(9)	124.5(3)
C(15)−Co(1)−Co(2)	50.83(7)	Co(1)−C(14)−Co(2)	79.16(10)
C(14)−Co(2)−C(15)	40.16(10)	Co(1)−C(15)−Co(2)	78.71(10)
C(13)−C(14)−C15)	139.6(2)	C(14)−C(15)−C16)	141.2(2)

Scheme 2

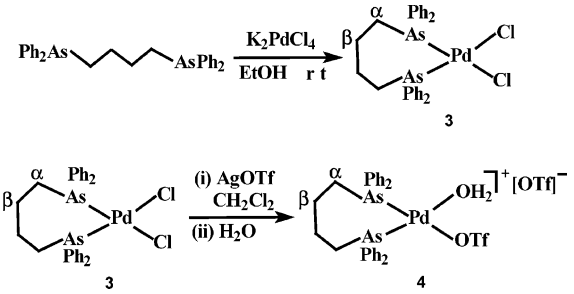

Complexes **3** and **4** are new and have been characterized by elemental analysis and spectroscopy. For example, the ^{1}H NMR spectrum of **3** displayed two singlets at 2.68 and 1.68 ppm for its α-CH_2 and β-CH_2 groups in the dpab ligand, whereas the spectrum of **4** showed two singlets at 2.55 and 2.16 ppm for its α-CH_2 and β-CH_2 groups in the dpab ligand. The ^{19}F NMR spectrum of **4** showed only one singlet at −78.80 ppm, although it has one coordinated OTf and one uncoordinated OTf group (see its crystal structure below). In addition, the ^{1}H NMR and IR spectra of **4** indicated the presence of H_2O by showing a broad singlet at 4.63 ppm and a broad absorption band at 3201 cm^{-1}, respectively.

The molecular structure of **4** was unambiguously established by crystal X-ray diffraction techniques. While Figure 2 shows its ORTEP drawing, Table 2 lists selected bond lengths and angles. X-ray diffraction confirmed that this molecule contains one $[OTf]^-$ anion and one $[Pd(dpab)(H_2O)(OTf)]^+$ cation. So, it is the first Pd(II) complex that contains one molecule of H_2O and one OTf as ligands, although numerous Pd(II) complexes usually contain either two molecules of H_2O or two OTf ligands.[4a,b] The Pd(1)−As(1) distance (2.3540(10) Å) is slightly longer than the Pd(1)−As(2) distance (2.3310(9) Å), whereas the Pd(1)−O(1) distance (2.145(3) Å) is

(10) (a) Dickson, R. S.; Fraser, P. J. *Adv. Organomet. Chem.* **1974**, *12*, 323. (b) Song, L.-C.; Wang, Z.-X.; Wang, J.-T.; Yao, X.-K.; Wang, H.-G. *Sci. China (Ser. B)* **1989**, *32*, 1281.
(11) Tzschach, A.; Lange, W. *Ber.* **1962**, *95*, 1360.

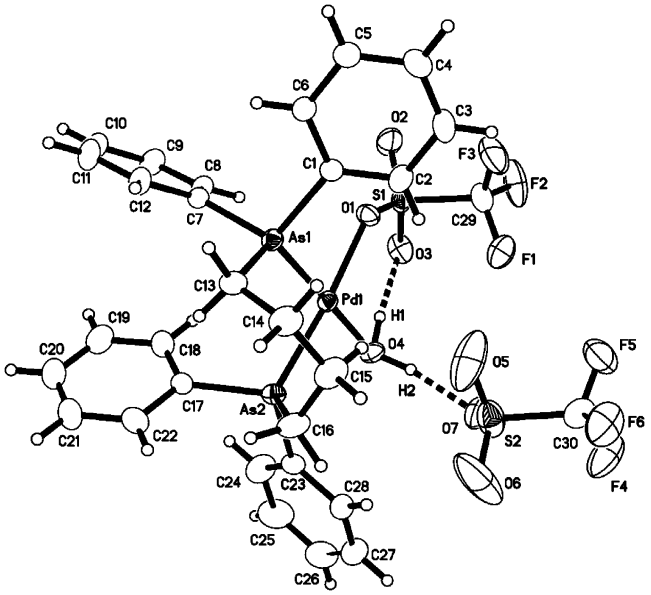

Figure 2. Molecular structure of **4** (thermal ellipsoids with 30% probability).

Table 2. Selected Bond Lengths (Å) and Angles (deg) for 4

Pd(1)−O(4)	2.121(3)	As(1)−C(13)	1.943(5)
Pd(1)−O(1)	2.145(3)	As(2)−C(17)	1.930(5)
Pd(1)−As(2)	2.3310(9)	S(1)−O(1)	1.465(3)
Pd(1)−As(1)	2.3540(10)	S(1)−C(29)	1.818(6)
As(1)−C(1)	1.930(5)	F(1)−C(29)	1.306(8)
O(4)−Pd(1)−O(1)	91.92(13)	C(1)−As(1)−C(7)	107.6(2)
O(1)−Pd(1)−As(2)	175.26(9)	O(2)−S(1)−O(1)	113.8(2)
O(1)−Pd(1)−As(1)	88.14(8)	O(1)−S(1)−C(29)	102.4(3)
As(1)−Pd(1)−As(2)	88.97(2)	S(1)−O(1)−Pd(1)	133.42(19)
C(1)−As(1)−C(13)	105.2(2)	F(1)−C(29)−S(1)	111.3(4)
O(4)−Pd(1)−As(2)	90.90(11)	C(1)−As(1)−Pd(1)	109.28(14)

slightly longer than the Pd(1)−O(4) distance (2.121(3) Å). The sum of bond angles O(4)−Pd(1)−O(1), O(4)−Pd(1)−As(2), O(1)−Pd(1)−As(1), and As(2)−Pd(1)−As(1) is exactly 360°, implying that Pd(1) adopts a square-planar coordination geometry. Figure 2 also shows that there are two types of intramolecular hydrogen bonding[12] in the solid state of complex **4**. The first one is the O(4)−H(1)···O(3) hydrogen bond, which is formed between the coordinated H_2O and the coordinated OTf, whose bond length and bond angle are 2.755 Å and 175.01°. Another one is O(4)−H(2)···O(7), which is formed between the coordinated H_2O and the uncoordinated OTf, whose bond length and bond angle are 2.702 Å and 169.36°, respectively. Obviously, the higher air and thermal stability of complex **4** compared to the intermediate bis(triflate) complex is due to the presence of such hydrogen bonding in monoaqua comlex **4**. In fact, the role of hydrogen bonding in the stabilization of the solid-state structure of aqua-transition metal complexes has long been recognized.[13]

Synthesis and Characterization of dpab-Chelated Pt(II) Complexes Pt(dpab)Cl_2 (5) and [Pt(dpab)$(H_2O)_2$][OTf]$_2$ (6). Similar to the preparation

Scheme 3

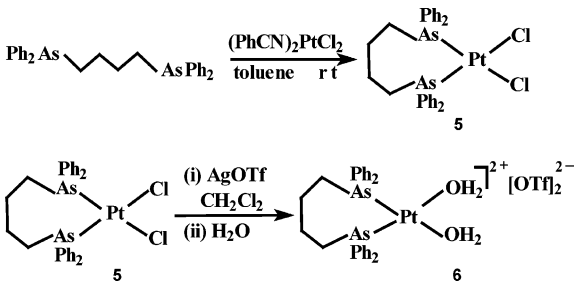

of complexes **3** and **4**, we also found that reaction of $(PhCN)_2PtCl_2$ with dpab in toluene at room temparature for 24 h afforded the Pt(II) dichloride complex **5** in 77% yield, whereas the Pt(II) diaqua complex **6** could be prepared by reaction of complex **5** with silver triflate in CH_2Cl_2 at room temperature followed by 10 min stirring in air (Scheme 3).

Although diphosphine-chelated Pt(II) complexes with a general formula of diphosphine PtX_2 (X = Cl, H_2O, OTf)[4a,b] are known, **5** and **6** are the first such diarsine-chelated Pt(II) complexes prepared so far. Complexes **5** and **6** are air-stable solids and have been characterized by elemental analysis and spectroscopy. The ^{1}H NMR spectrum of **5** showed two singlets at 2.69 and 1.69 ppm for its α-CH_2 and β-CH_2 groups in the dpab ligand, while the spectrum of **6** displayed two singlets at 2.74 and 1.87 ppm for its α-CH_2 and β-CH_2 groups in the dpab ligand. In addition, the IR spectrum of **6** displayed a broad band at 3054 cm^{-1}, indicating the presence of water. The ^{19}F NMR spectrum of **6** exhibited one singlet at −77.96 ppm for its two uncoordinated OTf groups. This singlet is just slightly shifted downfield compared to that caused by the two uncoordinated OTf groups in the diphosphine-chelated complex [Pt(dppf)$(H_2O)_2$][OTf]$_2$.[4b]

The structure of complex **6** was confirmed by crystal X-ray diffraction analysis. The ORTEP diagram of **6** is presented in Figure 3, whereas selected bond lengths and angles are listed in Table 3. As can be seen in Figure 3, the transition metal Pt(1) is attached to two

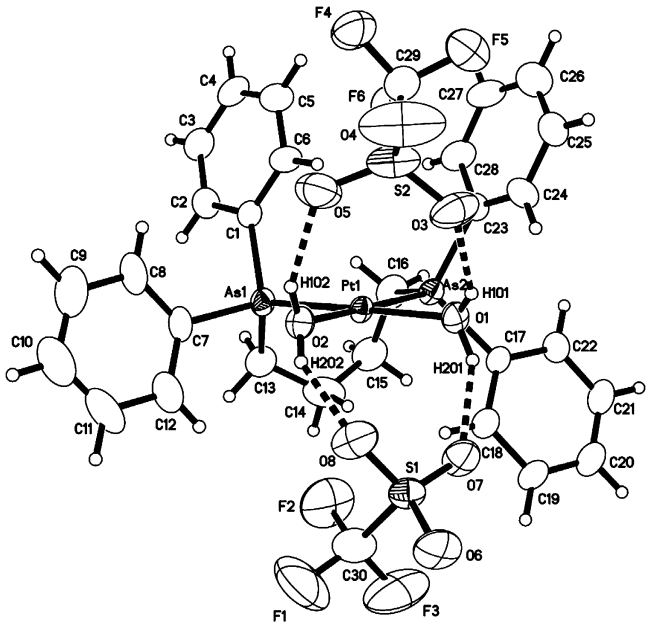

Figure 3. Molecular structure of **6** (thermal ellipsoids with 30% probability).

(12) Kollman, P. A.; Allen, L. C. *Chem. Rev.* **1972**, *72*, 283.
(13) See, for example: (a) Rochon, F. D.; Melanson, R. *Inorg. Chem.* **1987**, *26*, 989. (b) Britten, J. F.; Lippert, B.; Lock, C. J. L.; Pilon, P. *Inorg. Chem*. **1982**, *21*, 1936. (c) Hollis, L. S.; Lippard, S. J. *Inorg. Chem.* **1983**, *22*, 2605. (d) Braga, D.; Grepioni, F. *Acc. Chem. Res.* **1994**, *27*, 51. (e) Braga, D.; Grepioni, F.; Sabatino, P.; Desiraju, G. R. *Organometallics* **1994**, *13*, 3532.

Table 3. Selected Bond Lengths (Å) and Angles (deg) for 6

Pt(1)−O(1)	2.115(6)	As(1)−C(7)	1.926(10)
Pt(1)−O(2)	2.126(6)	As(2)−C(16)	1.935(10)
Pt(1)−As(2)	2.3272(10)	S(1)−O(6)	1.428(7)
Pt(1)−As(1)	2.3311(9)	S(1)−C(30)	1.776(14)
As(1)−C(1)	1.911(9)	F(1)−C(30)	1.284(19)
O(2)−Pt(1)−O(1)	87.1(2)	C(1)−As(1)−C(13)	107.1(5)
O(2)−Pt(1)−As(2)	174.06(17)	O(8)−S(1)−O(7)	111.5(5)
O(2)−Pt(1)−As(1)	92.00(17)	O(7)−S(1)−C(30)	104.3(8)
As(1)−Pt(1)−As(2)	93.40(4)	F(1)−C(30)−S(1)	112.1(13)
C(1)−As(1)−C(7)	106.3(4)	F(3)−C(30)−S(1)	110.6(11)
O(1)−Pt(1)−As(1)	178.99(17)	C(1)−As(1)−Pt(1)	112.2(3)

Scheme 4

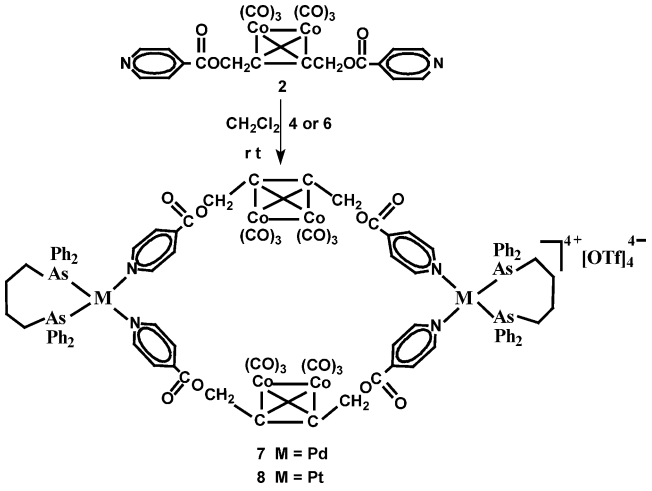

molecules of water through O(1) and O(2) and one molecule of dpab through As(1) and As(2). The Pt−As bond lengths are 2.3311(9) and 2.3272(10) Å, whereas the Pt−O bond lengths are 2.115(6) and 2.126(6) Å, respectively. The bond angle around Pt(1) is exactly 360°, which means that the geometry of Pt(1) is square-planar. This molecule contains two uncoordinated counteranions $[OTf]^-$, which interact with the cation $[Pt(dpab)(H_2O)_2]^+$ through four identical intramolecular hydrogen bonds[12] formed between the two coordinated H_2O and the two uncoordinated OTf groups (Figure 3). The bond lengths of these hydrogen bonds are O(1)−H(101)···O(3) = 2.620 Å, O(1)−H(201)···O(7) = 2.656 Å, O(2)−H(102)···O(5) = 2.683 Å, and O(2)−H(202)···O(8) = 2.676 Å, whereas the bond angles of these hydrogen bonds are equal to 145.1°, 147.7°, 150.4°, and 151.5°, respectively. Similar to the monoaqua complex **4**, diaqua complex **6**, due to having such hydrogen bonding, is much more stable than its bis(triflate) complex.[13]

Synthesis and Characterization of Metal Cluster-Containing Macrocycles {[M(dpab)]-μ-[(4-C_5H_4-$NCO_2CH_2)_2C_2Co_2(CO)_6$]}$_2$[OTf]$_4$ (7, M = Pd; 8, M = Pt). More interestingly, we found that the tetrahedral Co_2C_2 cluster-bridged bipyridine ligand **2** could undergo self-assembly reaction with monoaqua Pd(II) complex **4** or diaqua Pt(II) complex **6** in dichloromethane at room temperature to give the corresponding tetrahedral cluster-containing metallomacrocycles **7** and **8** in 93% and 85% yields, respectively (Scheme 4).

Complexes **7** and **8** are air-stable solids, which have been fully characterized by elemental analysis, spectroscopy, and X-ray diffraction study. The IR spectra of **7** and **8** showed three strong absorption bands in the range 2100−2032 cm^{-1} for their terminal carbonyls and

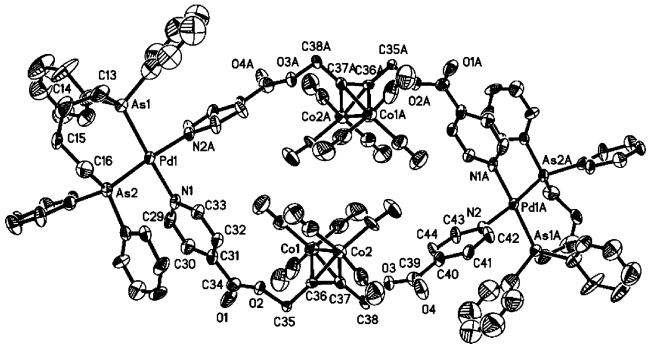

Figure 4. Molecular structure of cationic macrocycle of **7** (thermal ellipsoids with 30% probability).

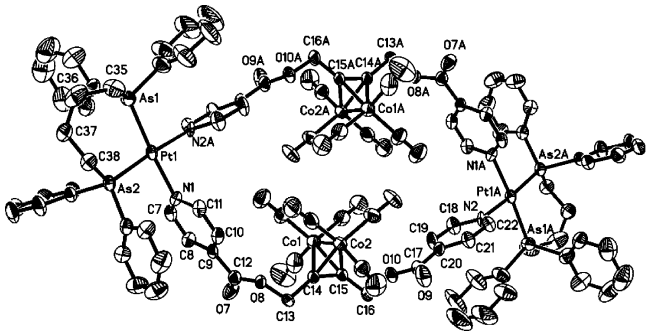

Figure 5. Molecular structure of cationic macrocycle of **8** (thermal ellipsoids with 30% probability).

Table 4. Selected Bond Lengths (Å) and Angles (deg) for 7 and 8

7

Pd(1)−As(2)	2.374(2)	Pd(1)−As(1)	2.387(2)
Co(1)−C(36)	1.906(13)	Pd (1)−N(1)	2.070(11)
As(1)−C(13)	1.939(15)	Co(1)−C(37)	1.949(14)
As(2)−C(16)	1.939(13)	Co(1)−Co(2)	2.462(3)
O(1)−C(34)	1.174(15)	N(1)−C(29)	1.325(15)
C(36)−C(37)	1.322(16)	O(2)−C(34)	1.348(16)
N(1)−Pd(1)−N(2A)	87.0(4)	C(36)−Co(1)−Co(2)	51.2(4)
N(1)−Pd(1)−As(2)	88.9(3)	C(36)−Co(2)−C(37)	39.4(5)
N(1)−Pd(1)−As(1)	177.5(3)	C(37)−Co(2)−Co(1)	50.7(4)
As(1)−Pd(1)−As(2)	93.60(7)	C(33)−N(1)−C(29)	117.8(12)
C(45)−Co(1)−C(36)	98.2(8)	C(36)−Co(1)−C(37)	40.1(5)

8

Pt(1)−As(2)	2.3733(18)	Pt(1)−As(1)	2.3746(17)
Co(1)−C(14)	1.972(11)	Pt(1)−N(1)	2.138(8)
As(1)−C(35)	1.916(14)	Co(1)−C(15)	1.961(11)
As(2)−C(38)	1.939(11)	Co(1)−Co(2)	2.451(3)
O(7)−C(12)	1.192(15)	N(1)−C(7)	1.282(13)
C(14)−C(15)	1.335(14)	O(8)−C(12)	1.331(14)
N(1)−Pt(1)−N(2A)	87.5(3)	C(14)−Co(1)−Co(2)	50.7(3)
N(1)−Pt(1)−As(2)	88.5(2)	C(15)−Co(2)−C(14)	40.2(4)
N(1)−Pt(1)−As(1)	176.0(2)	C(15)−Co(2)−Co(1)	51.4(3)
As(1)−Pt(1)−As(2)	94.97(5)	C(7)−N(1)−C(11)	123.6(10)
C(1)−Co(1)−C(14)	139.2(6)	C(15)−Co(1)−C(14)	39.7(4)

one strong absorption band at 1738 cm^{-1} for their ester carbonyls. The presence of triflate counterions in **7** and **8** is indicated by one singlet in their ^{19}F NMR spectra at −78.26 and −77.11 ppm, respectively. Thus, the ^{19}F NMR behavior of the triflates in **7** and **8** is very close to that of the triflates in their precursors **4** and **6** and even those of the diphosphine-chelated Pd(II) and Pt(II) complexes.[4a,b]

Figures 4 and 5 show the ORTEP diagrams of the cationic parts of **7** and **8**, while selected bond lengths and angles are given in Tables 4 and 5, respectively. In fact, **7** and **8** are isostructural, and their macrocyclic

Table 5. Crystal Data and Structural Refinement Details for 2, 4, and 6

	2	**4**	**6**
mol formula	$C_{22}H_{12}Co_2N_2O_{10}$	$C_{30}H_{30}As_2F_6O_7PdS_2$	$C_{30}H_{32}As_2F_6O_8PtS_2{\cdot}CH_2Cl_2$
mol wt	582.20	936.90	1128.53
temp/K	293(2)	293(2)	293(2)
cryst syst	triclinic	monoclinic	monoclinic
space group	$P\bar{1}$	P2(1)/*n*	P2(1)/*n*
a/Å	8.958(3)	10.113(3)	11.4180(13)
b/Å	11.630(4)	31.297(11)	21.677(3)
c/Å	13.370(4)	11.349(4)	16.1975(18)
α/deg	64.807(5)	90	90
β/deg	79.845(6)	106.385(6)	92.132(2)
γ/deg	70.453(5)	90	90
V/Å^3	1187.0(7)	3446(2)	4006.2(8)
Z	2	4	4
D_c/g·cm^{-3}	1.629	1.806	1.871
abs coeff/mm^{-1}	1.457	2.642	5.452
cryst size/mm	0.30 × 0.25 × 0.15	0.30 × 0.25 × 0.20	0.22 × 0.18 × 0.08
F(000)	584	1856	2192
$2\theta_{max}$/deg	50.06	50.70	50
no. of reflns	4972	11 545	20 742
no. of indep reflns	4172 (R_{int} = 0.0180)	6263 (R_{int} = 0.0400)	7053 (R_{int} = 0.1505)
index ranges	$-10 \le h \le 9$	$-10 \le h \le 12$	$-12 \le h \le 13$
	$-13 \le k \le 12$	$-37 \le k \le 28$	$-14 \le k \le 25$
	$-11 \le l \le 15$	$-13 \le l \le 7$	$-17 \le l \le 19$
scan type	$\omega-2\theta$	$\omega-2\theta$	$\omega-2\theta$
no. of data/restraints/params	4172/0/325	6263/3/441	7053/6/473
goodness of fit on F^2	0.930	0.969	0.937
R	0.0322	0.0435	0.0584
R_w	0.0693	0.0756	0.1372
largest diff peak and hole/e Å^{-3}	0.320/−0.316	0.681/−0.584	3.831/−2.826

cations each contain two dpab-chelated transition metal Pd or Pt moieties that are held together by two molecules of the tetrahedral Co_2C_2 cluster-bridged bipyridine ligands. The coordination geometry around Pd(1)/Pd(1A) or Pt(1)/Pt(1A) metal centers is normal square-planar with slight deviations of the bond angles. All Pd−As or Pt−As distances are normal within the range 2.374−2.387 or 2.373−2.375 Å, respectively. Likewise, the Pd−N and Pt−N distances are normal with the region 2.070−2.092 Å or 2.126−2.138 Å, whereas the N−Pd−N and N−Pt−N angles are 87.0(4)° or 87.5(3)°, respectively. In fact, the geometric parameters of **7** and **8** are comparable with those for other Pd(II) and Pt(II) macrocycles containing bidentate N ligands.[4a,7] The additional important geometric features for **7** and **8** are that (i) both molecules are centrosymmetric, (ii) the two pyridinde rings in each bipyridine ligand **2** of **7** or **8** are cis to the $Co_2(CO)_6$ moiety of the tetrahedral Co_2C_2 cluster unit, (iii) the four pyridine rings and the Co(1)−Co(2)−Co(1A)−Co(2A) plane in **7** and **8** are nearly perpendicular to the plane defined by the six atoms Pd(1), C(36), C(37), Pd(1A), C(36A), and C(37A) in **7** or the six atoms Pt(1), C(14), C(15), Pt(1A), C(14A), and C(15A) in **8** respectively, and (iv) the two Pd or two Pt atoms and the four Co atoms in **7** and **8** are located at six apical positions of an octahedron. It follows that the structures of **7** and **8**, in contrast to those metallomacycles without cluster-bridged N donor ligands,[4−7] are unique and unprecedented.

Conclusions

We have first synthesized and characterized the tetrahedral Co_2C_2 cluster-bridged bipyridine ligand **2** and the diarsine dpab-chelated Pd(II)/Pt(II) complexes **3**−**6**. Study on self-assembly of ligand **2** with complex **4** or **6** has allowed us to obtain two metallomacrocyclic compounds **7** and **8**, which contain the corresponding Co_2C_2 cluster cores and represent a unique and interesting class of metallomacrocycles. Further studies on the possible new properties caused by the Co_2C_2 cluster cores[10a] in **7** and **8** and the self-assembly reactions of either bipyridine ligand **2** with other metal complexes or complexes **4** and **6** with other cluster-bridged bipyridine ligands are in progress in this laboratory.

Experimental Section

General Comments. All reactions were carried out under highly purified nitrogen atmosphere using standard Schlenk or vacuum-line techniques. Solvents for preparative use were dried and distilled under nitrogen from CaH_2 or sodium/benzophenone ketyl prior to use. All solvents were bubbled for at least 15 min before use. 1,4-Dibromobutane, K_2PdCl_4, silver triflate, and $Co_2(CO)_8$ were of commercial origin and used as received. 4-Pyridinecarboxylic acid 2-butyne-1,4-diyl ester,[14] Ph_2AsCl,[15] and $(PhCN)_2PtCl_2$[16] were prepared according to literature methods. ^{1}H NMR spectra were recorded on a Bruker AC-P 200 or a Bruker 300M NMR spectrometer, and chemical shifts are reported in ppm relative to internal Me_4Si (δ = 0). ^{19}F NMR spectra were measured on a Bruker 300M spectrometer, and chemical shifts are referenced relative to external CF_3CO_2D (δ = 0). IR spectra were taken on a Bio-Rad FTS 135 spectrophotometer. Elemental analysis was performed on an Elementar Vario EL analyzer, and melting points were determined on a Yanaco MP-500 melting point apparatus.

Improved Preparation of $Ph_2As(CH_2)_4AsPh_2$ (dpab).[11] A Schlenk flask was charged with 0.1 g (14.4 mmol) of lithium and 20 mL of diethyl ether. Under stirring, the mixture was cooled to −40 °C and then a solution of 0.41 mL (3.5 mmol) of 1,4-dibromobutane in 20 mL of diethyl ether was slowly added.

(14) (a) Moser, U.; Gubitz, C.; Galvan, M.; Immel-Sehr, A.; Lambrecht, G.; Mutschler, E. *Arzneim.-Forsch.* **1995**, *45*, 449. (b) Badgett, C. O.; Woodward, C. F. *J. Am. Chem. Soc.* **1947**, *69*, 2907.

(15) Barker, R. L.; Booth, E.; Jones, W. E.; Woodward, F. N. *J. Soc. Chem. Ind.* **1949**, *68*, 277.

(16) Uchiyama, T.; Toshiyasu, Y.; Nakamura, Y.; Miwa, T.; Kawaguchi, S. *Bull. Chem. Soc. Jpn.* **1981**, *54*, 181.

Table 6. Crystal Data and Structural Refinement Details for 7 and 8

	7	8
mol formula	$C_{104}H_{80}As_4Co_4F_{12}N_4O_{32}Pd_2S_4$	$C_{104}H_{80}As_4Co_4F_{12}N_4O_{32}Pt_2S_4 \cdot 8.5H_2O$
mol wt	3002.16	3338.68
temp/K	293(2)	293(2)
cryst syst	triclinic	triclinic
space group	$P\bar{1}$	$P\bar{1}$
a/Å	13.696(8)	13.667(9)
b/Å	14.648(8)	17.272(11)
c/Å	17.666(11)	18.060(12)
α/deg	77.777(11)	92.019(12)
β/deg	76.557(11)	101.885(11)
γ/deg	73.831(12)	104.029(11)
V/Å^3	3269(3)	4031(5)
Z	1	1
D_c/g·cm^{-3}	1.523	1.373
abs coeff/mm^{-1}	1.919	3.074
cryst size/mm	0.16 × 0.14 × 0.08	0.38 × 0.34 × 0.18
F(000)	1492	1641
$2\theta_{max}$/deg	50.02	52.82
no. of reflns	16 932	23 261
no. of indep reflns	11 379 (R_{int} = 0.1011)	16 267 (R_{int} = 0.0452)
index ranges	$-16 \le h \le 15$ $-13 \le k \le 17$ $-21 \le l \le 21$	$-17 \le h \le 16$ $-20 \le k \le 21$ $-18 \le l \le 22$
scan type	$\omega-2\theta$	$\omega-2\theta$
no. of data/restraints/params	11 379/67/736	16 267/147/828
goodness of fit on F^2	1.000	1.041
R	0.0949	0.0689
R_w	0.1608	0.2004
largest diff peak and hole/e Å^{-3}	0.968/−0.604	1.349/−1.738

After the new mixture was warmed to room temperature and stirred for 18 h, it was filtered to give a filtrate containing 1,4-dilithiumbutane.[17] The filtrate was cooled to −20 °C, and then 1 mL (5.57 mmol) of Ph_2AsCl was added. The new mixture was warmed to room temperature and stirred at this temperature for 12 h. To this mixture was added 10 mL of water, and the resulting mixture was stirred for an additional 0.5 h. The organic layer was separated, washed twice with water, and dried over anhydrous $MgSO_4$. After removal of $MgSO_4$ and solvent, the residue was recrystallized from diethyl ether to give 1.32 g (73%) of dpab as a white solid.

Preparation of (4-$C_5H_4NCO_2CH_2)_2C_2Co_2(CO)_6$ (2). A Schlenk flask was charged with 0.445 g (1.5 mmol) of 4-pyridinecarboxylic acid 2-butyne-1,4-diyl ester and 30 mL of petroleum ether. While stirring, a solution of 0.514 g (1.5 mmol) of $Co_2(CO)_8$ in 15 mL of petroleum ether was slowly added. The mixture was stirred at room temperature for an additional 2−3 h until no CO evolution was observed. Solvent was removed under reduced pressure, and the residue was subjected to column chromatography (alkali Al_2O_3) using $CHCl_3$ as eluent. The crude product obtained from the eluted red band was recrystallized from CH_2Cl_2/petroleum ether to give 0.747 g (86%) of **2** as a red solid. Mp: 130 °C dec. Anal. Calcd for $C_{22}H_{12}Co_2N_2O_{10}$: C, 45.39; H, 2.08; N, 4.81. Found: C, 45.29; H, 1.93; N, 5.04. IR (KBr disk): $\nu_{C\equiv O}$ 2105 (s), 2066 (s), 2026 (vs), 1993 (s); $\nu_{C=O}$ 1728 (s) cm^{-1}. ^{1}H NMR (200 MHz, $CDCl_3$): δ 9.18 (br s, 4H, 4H$_\alpha$), 7.95 (br s, 4H, 4H$_\beta$), 5.55 (s, 4H, 2CH_2). ^{13}C NMR (50.3 MHz, $CDCl_3$): δ 197.66 (C≡O), 164.43 (CO_2), 142.53 (C$_\alpha$), 135.67 (C$_\gamma$), 132.92 (C$_\beta$), 87.67 (CCo), 65.29 (CH_2).

Preparation of Pd(dpab)Cl_2 (3). A Schlenk flask was charged with 0.204 g (0.63 mmol) of K_2PdCl_4, 0.308 g (0.60 mmol) of dpab, and 16 mL of anhydrous ethyl alcohol. The mixture was stirred for 1 h at room temperature to give a yellowish precipitate. The precipitate was sequentially washed with water, ethyl alcohol, and diethyl ether and finally dried in a vacuum to give 0.374 g (90%) of **3** as a light yellow solid. Mp >300 °C. Anal. Calcd for $C_{28}H_{28}As_2Cl_2Pd$: C, 48.62; H, 4.08. Found: C, 48.66; H, 3.95. IR (KBr disk): 3055 (m), 2920 (m), 2851 (w), 1578 (m), 1483 (s), 1436 (vs) 1308 (m), 1082 (s), 893 (s), 736 (vs) 692 (vs), 561 (m) cm^{-1}. ^{1}H NMR (300 MHz, DMSO-d_6): δ 7.75, 7.51 (2 br s, 20H, 4C_6H_5), 2.68 (s, 4H, 2CH_2As), 1.68 (s, 4H, 2CH_2).

Preparation of [Pd(dpab)(H_2O)(OTf)][OTf] (4). To a suspension of 0.126 g (0.18 mmol) of Pd(dpab)Cl_2 in 35 mL of CH_2Cl_2 was added 0.138 g (0.54 mmol) of AgOTf, and then the mixture was stirred at room temperature for 24 h with the exclusion of light. The resulting mixture was filtered to give a filtrate, which was stirred in air for 10 min and then was reduced to ca. 2 mL at reduced pressure. Diethyl ether was added to give a precipitate, which was washed with diethyl ether and dried in a vacuum to give 0.053 g (93%) of **4** as a yellow solid. Mp: 196−198 °C dec. Anal. Calcd for $C_{30}H_{30}As_2F_6O_7PdS_2$: C, 38.46; H, 3.23. Found: C, 38.98; H, 3.10. IR (KBr disk): ν_{OH} 3201 (m); ν_{OTf} 1288 (vs), 1237 (vs), 1162 (s), 1030 (vs) cm^{-1}. ^{1}H NMR (200 MHz, $CDCl_3$): δ 7.58−7.41 (m, 20H, 4C_6H_5), 4.63 (br s, 2H, H_2O), 2.55 (s, 4H, 2CH_2As), 2.16 (s, 4H, 2CH_2). ^{19}F NMR (282 MHz, $CDCl_3$): δ −78.80 (s, SO_3CF_3).

Preparation of Pt(dpab)Cl_2 (5). A mixture of 0.32 g (0.678 mmol) of $(PhCN)_2PtCl_2$, 0.348 g (0.678 mmol) of dpab, and 16 mL of toluene was stirred at room temperature for 24 h to give a white precipitate. The precipitate was washed successively with toluene and diethyl ether and then dried in a vacuum to afford 0.406 g (77%) of **5** as a white powder. Mp: 300 °C (dec). Anal. Calcd for $C_{28}H_{28}As_2Cl_2Pt$: C, 43.10; H, 3.62. Found: C, 43.22; H, 3.61. IR (KBr disk): 3054 (m), 2919 (m), 2853 (w), 2036 (w), 1984 (m), 1578 (m), 1483 (s), 1436 (vs) 1309 (m), 1082 (s), 894 (s), 738 (vs), 692 (vs), 471 (vs) cm^{-1}. ^{1}H NMR (300 MHz, DMSO-d_6): δ 7.74, 7.52 (2 br s, 20H, 4C_6H_5), 2.69 (s, 4H, 2CH_2As), 1.69 (s, 4H, 2CH_2).

Preparation of [Pt(dpab)(H_2O)$_2$][OTf]$_2$ (6). By a procedure similar to that described in the preparation of **4**, 0.191 g (88%) of **6** as a white solid was obtained from 0.166 g (0.213 mmol) of Pt (dpab)Cl_2, 0.137 g (0.532 mmol) of AgOTf, and 20 mL of CH_2Cl_2. Mp: 178−180 °C. Anal. Calcd for $C_{30}H_{32}As_2F_6O_8PtS_2$: C, 34.53; H, 3.09. Found: C, 34.56; H, 3.25. IR (KBr disk): ν_{OH} 3054 (m); ν_{OTf} 1253 (vs), 1170 (vs), 1031 (vs) cm^{-1}. ^{1}H NMR (300 MHz, DMSO-d_6): δ 7.57−7.78 (m, 20H,

(17) West, R.; Rochow, E. G. *J. Org. Chem.* **1953**, *18*, 1739.

$4C_6H_5$), 2.74 (s, 4H, $2CH_2As$), 1.87 (s, 4H, $2CH_2$). ^{19}F NMR (282 MHz, acetone-d_6): δ −77.96 (s, SO_3CF_3).

Preparation of {[Pd(dpab)]-μ-[(4-$C_5H_4NCO_2CH_2)_2C_2Co_2(CO)_6$]}$_2$[OTf]$_4$ (7). A Schlenk flask was charged with 0.058 g (0.062 mmol) of [Pd(dpab)(H_2O)(OTf)][OTf], 0.056 g (0.062 mmol) of (4-$C_5H_4NCO_2CH_2)_2C_2Co_2(CO)_6$, and 20 mL of CH_2Cl_2. The mixture was stirred at room temperature for 24 h to produce a red precipitate. The precipitate was washed with CH_2Cl_2 and recrystallized from a mixture of CH_3CN and diethyl ether to give 0.085 g (92%) of **7** as a red solid. Mp: 165 °C dec. Anal. Calcd for $C_{104}H_{80}As_4Co_4F_{12}N_4O_{32}Pd_2S_4$: C, 41.60; H, 2.69; N, 1.87. Found: C, 41.25; H, 3.11, N, 2.13. IR (KBr disk): $\nu_{C\equiv O}$ 2099 (s), 2063 (vs), 2036 (vs); $\nu_{C=O}$ 1738 (s); ν_{OTf} 1275 (vs), 1223 (s), 1159 (s), 1029 (s) cm^{-1}. ^1H NMR (200 MHz, $CDCl_3$): δ 7.64−7.38 (m, 56H, $8C_6H_5$, $4C_5H_4N$), 5.28 (s, 8H, $4CH_2O$), 2.38 (s, 8H, $4CH_2As$), 1.97 (s, 8H, $4CH_2$). ^{19}F NMR (282 MHz, acetone-d_6): δ −78.26 (s, SO_3CF_3).

Preparation of {[Pt(dpab)]-μ-[(4-$C_5H_4NCO_2CH_2)_2C_2Co_2(CO)_6$]}$_2$[OTf]$_4$ (8). In a manner similar to that described for the preparation of **7**, 0.092 g (85%) of **8** as a red solid was prepared from 0.07 g (0.068 mmol) of [Pt(dpab)(H_2O)$_2$][OTf]$_2$ and 0.04 g (0.068 mmol) of (4-$C_5H_4NCO_2CH_2)_2C_2Co_2(CO)_6$. Mp: 140 °C dec. Anal. Calcd for $C_{104}H_{80}As_4Co_4F_{12}N_4O_{32}Pt_2S_4$: C, 39.29; H, 2.54; N, 1.76. Found: C, 39.30; H, 2.47; N, 1.76. IR (KBr, disk): $\nu_{C\equiv O}$ 2100 (s), 2063 (vs), 2032 (vs); $\nu_{C=O}$ 1738 (s); ν_{OTf} 1279 (s), 1225 (s), 1158 (s), 1030 (s) cm^{-1}. ^1H NMR (300 MHz, DMSO-d_6): δ 9.02 (d, J = 5.70 Hz, 8H, $8H_\alpha$), 7.73 (d, J = 5.70 Hz, 8H, $8H_\beta$), 7.74−7.43 (m, 40H, $8C_6H_5$), 5.62 (s, 8H, $4CH_2O$), 3.06 (s, 8H, $4CH_2As$), 1.87 (s, 8H, $4CH_2$). ^{19}F NMR (282 MHz, DMSO-d_6): δ −77.11 (s, SO_3CF_3).

X-ray Structure Determinations of 2, 4, 6, 7, and 8. X-ray quality single crystals of **2** were grown by slow evaporation of its dichloromethane/petroleum ether solution at 4 °C, whereas those of **4** and **6** were obtained by slow diffusion of diethyl ether or hexane into their dichloromethane solutions at room temperature, respectively. While the single crystals of **7** were grown by slow diffusion of diethyl ether into its nitromethane solution containing several drops of glacial acetic acid at room temperature, those of **8** were produced by slow diffusion reaction of an acetone solution of ligand **2** into a dichloromethane solution of complex **6** under nitrogen at room temperature. However, since the single crystals of **8** are highly effloresent even under nitrogen, they must be sealed with great care in a capillary immediately after being taken out from the crystal-growing solvent system. Each crystal suitable for X-ray diffraction analysis was mounted on a Bruker SMART 1000 automated diffractometer. Data were collected at 293(2) K using Mo Kα graphite-monochromated radiation (λ = 0.71073 Å) in the ω scanning mode. Absorption corrections were performed using SADABS. The structures were solved by direct methods using the SHELXTL-97 program. The final refinements were accomplished by the full-matrix least-squares method with anisotropic thermal parameters for non-hydrogen atoms. All hydrogen atoms were located by using the geometric method. Details of the crystal data, data collections, and structure refinements are summarized in Tables 5 and 6, respectively.

Acknowledgment. We are grateful to the National Natural Science Foundation of China and the Research Fund for the Doctoral Program of Higher Education of China for financial support.

Supporting Information Available: All crystal data, atomic coordinates, thermal parameters, and bond lengths and angles for **2**, **4**, **6**, **7**, and **8** as CIF files. This material is available free of charge via the Internet at http://pubs.acs.org.

OM049175Y